Microspheres for Local Drug Delivery

Zandstra, Jurjen

Chapter 4

Biocompatibility of monodisperse microspheres composed of a biodegradable poly(DL-lactide-PEG)-b-poly(L-Lactide) multiblock copolymer

(A possible replacement for PLGA drug release for proteins)

J. Zandstra, M.M. van Beuge, C. Hiemstra, A.H. Petersen, J. Zuidema, A.A.R. Lathuile, G.J. Veldhuis, R. Steendam, R.A. Bank, E.R. Popa

Abstract

The increasing prevalence and treatment costs of chronic kidney disease call for novel therapeutic strategies that prevent disease progression at an early stage. We propose polymer microspheres (MSP) with physical and chemical properties tailored to controlled intrarenal drug delivery as a tool to modulate processes responsible for chronic kidney disease, such as inflammation and fibrosis. In this study we generated polydisperse and monodisperse, hydrophilic-phase-separated-multiblock copolymer-based (SynBiosys 50LP10) MSP and investigated their *in vitro*, subcutaneous and intrarenal biocompatibility and thus adequacy for future therapeutic application.

Monodisperse and polydisperse SynBiosys MSP showed excellent cytocompatibility properties upon 72 hour incubation with three different cell types. A mild foreign body was observed as indicated by a minimum presence of macrophages and myofibroblasts which was slightly enhanced against small microspheres.

MSP were detected in the subcapsular space at all time points and showed little degradation in time. MSP implantation did not affect tubular integrity at any time point. Macrophages and myofibroblasts were virtually absent in the renal interstitium. Based on their slow degradation rate and the lack of adverse effects of their subcapsular implantation on the renal tissue, we propose monodisperse MSP to be a promising tool for sustained, controlled intrarenal drug delivery. Because of the drawbacks of PLGA MSP, SynBiosys MSP might be a good substitute for controlled local protein drug delivery.

Introduction

Poly(D,L-lactic-co-glycolic acid) (PLGA) is a biodegradable polymer which is considered to be biocompatible by the FDA. The use of PLGA has been investigated for a wide variety of purposes such as controlled delivery of low molecular weight drugs [1-3], proteins [4-6] and vaccine antigens [7,8]. PLGA is degraded by a process called hydrolysis where the ester bond is broken down and lactic acid and glycolic acid are formed [9,10]. The buildup of these naturally occurring acids during degradation is an important drawback of the use of PLGA as a drug delivery vehicle, because the acidic local microenvironment that is formed is harmful to proteinaceous drugs entrapped within the polymer [11,12]. Denaturation of the formulated protein or structural modifications due to acid-catalyzed reactions can not only affect the therapeutic efficacy of the protein, but can also cause potential immunological responses to the formulated protein[13,14].

By designing a new block copolymer based on poly(DL-lactide)-PEG1000-poly(DL-lactide) and poly(L-lactide), we aim to avoid the drawbacks of PLGA-based materials, while still retaining the advantageous release profile. This polymer, designated SynBiosys 50LP10, is expected to have the same release profile as PLGA, but will not degrade into acidic components.

Currently many forms of drug delivery products exist, such as minipumps, rods, gels and microspheres. All of these have their own drawbacks and pitfalls [15]. We are aiming for a biomaterial which is injectable, biodegradable and capable of releasing a drug gradually over time. This drug delivery vehicle can then be used in multiple disease

systems and is therefore multifunctional. Starting from these desired characteristics we chose to develop a microsphere (MSP) since the other options do not comply with the requirements outlined above. Minipumps are not biodegradable, rods are not easily injected and gels have difficulty releasing drugs for a prolonged period of time.

Previously, we have shown that MSP size influences the foreign body response (FBR) [16]. The FBR is an immune response against a foreign body material aimed at encapsulation or degradation of the foreign body material. We have shown this using polydisperse, 5 μm, and 30 μm PLGA microspheres, and found that 30 μm mMSP caused a milder FBR. In the current study we investigated whether we could confirm these findings with our novel polymer in order to exclude that our previous findings were specific to the polymer used. Therefore, we first investigated whether the new synbiosys 50LP10 polymer MSP were biocompatible in a subcutaneous foreign body reaction model and subsequently whether these MSP are a suitable candidate for local drug delivery in organs.

As a model organ we chose the kidney to investigate whether local drug delivery in organs is possible. For this to be the case these MSP should evoke a moderate FBR, and cause no additional damage to the kidney (in particular the kidney cortex) during the implantation procedure.

In this study we investigated the distribution and biocompatibility of synbiosys 50LP10 MSP injected underneath the kidney capsule and subcutaneously. We used conventional polydisperse MSP and monodisperse 5 μm and 30 μm MSP (mMSP) for these experiments to further investigate the FBR against mMSP compared to polydisperse MSP.

Materials and methods

Chemicals

SynBiosys 20[PDLA-PEG_{1000}]-80[PLLA], a multiblock copolymer consisting of 20% w/w of poly(DL-lactide)-PEG1000-poly(DL-lactide) with a molecular weight of 2000 g/mole and 80% w/w of poly(L-lactide) with a molecular weight of 4000 g/mole was synthesized by InnoCore Pharmaceuticals (Groningen, The Netherlands), see below. Polyvinyl alcohol (PVA 13-23) was purchased from Aldrich (Zwijndrecht, The Netherlands). Dichloromethane (DCM, p.a. stabilized with EtOH), sodium azide (NaN_3) and Tween-20 were purchased from Across (Geel, Belgium). Sodium dodecyl sulphate (SDS) was purchased from Sigma-Aldrich (Zwijndrecht, The Netherlands). Potassium chloride (KCl), sodium chloride (NaCl), potassium dihydrogen orthophosphate (KH2PO4), disodium hydrogen phosphate (Na_2HPO_4) were purchased from Fisher Scientifics (Leicestershire, UK).

Synthesis of 20[PDLA-PEG_{1500}]-b-80[PLLA] multi-block copolymers

Low molecular weight poly(L-Lactide) [PLLA] (Mw 4000 g/mol) and poly(DL-Lactide)-PEG_{1000}-poly(DL-Lactide) [PDLA-PEG_{10500}] (Mw 2000 g/mol) prepolymers were synthesized by standard stannous octoate catalysed ring-opening polymerization, using procedures similar to those described previously. PLLA and PDLA-PEG_{1000}prepolymers were then chain-extended in dioxane with 1,4-butanediisocyanate to prepare $[PDLA\text{-}PEG_{1000}]_{2000}$-b-$[PLLA]_{4000}$multiblock co-polymers with a [PDLA-PEG_{1500}] / [PLLA] block ratio of 20 /80 w/w (abbreviated as

20[PDLA-PEG_{1000}]-80[PLLA]). After cooling to room temperature, the reaction mixture was freeze-dried at 30 ˚C to remove 1,4-dioxane.

Microsphere preparation

Monodisperse MSP (monospheres) were prepared by a membrane emulsification-based solvent extraction/evaporation process using an Iris-20 microsieve membrane with uniformly sized pores of 20 micron (Nanomi BV, The Netherlands).

For MSP approximately 3.0 g of 20[PDLA-PEG_{1500}]-80[PLLA] polymer was dissolved in 9 mL dichloromethane (DCM) to obtain a 20 % w/w solution and filtered through a 0.2 mm PTFE filter. The filtered polymer solution was processed through the microsieve membrane using 35 mbar air-pressure into an aqueous solution containing 4 % w/v polyvinylalcohol (PVA) as emulsifier thereby forming a dispersion of mMSP. The formed dispersion was stirred for at least 3 hours at room temperature to extract and evaporate the solvent. The hardened MSP were concentrated by filtration and washed repeatedly with ultrapure water containing 0.05% Tween 20 and finally lyophilized. mMSP were stored at -20°C until evaluation.

Microsphere characterization

mMSP were visually examined and measured by optical microscopy.

Extraction of leachables from 50LP10 MSP

To extract leachables (e.g. solvent residues, low molecular weight oligomers, catalyst residues) from these polymers, 50LP10 MSP (0.17

mg/mL) were shaken for 24h at 37°C in complete culture medium in a pyrogen-free tube. The negative control polymer polyurethane (PU) and positive control rubber latex were treated similarly. Subsequently, solid material and supernatant were separated by centrifugation at 1250rpm (300g). The supernatant was immediately used for *in vitro* biocompatibility assays.

Cells and culture media

Human skin fibroblasts (PK-84) were cultured in RPMI 1640 medium, supplemented with 10% fetal calf serum (FCS), 1% glutamine, 1% penicillin and 1% streptomycin. The human proximal tubular cell line HK2 was cultured in 1:1 Ham's F12 (L-glutamin) and DMEM supplemented with 10% FCS, 1% glutamine, 1% penicillin, 0.01 mg/L EGF, 10mg/L insulin, 5.5mg/L transferrin, 6.7 µg/L sodium selenite, 36ug/L hydrocortisone and 2mM glutamax. Primary human tubular epithelial cells (PTEC) were cultured in 1:1 Ham's F12 (L-glutamin) and DMEM supplemented with 1% human pooled serum, 1% glutamine, 1% penicillin, 0.01 mg/L EGF, 10mg/L insulin, 5.5mg/L transferrin, 6.7 µg/L sodium selenite, 36ug/L hydrocortisone and 2mM glutamax. All cell cultures were incubated at 37°C, 5% CO_2.

In vitro biocompatibility assays

To test the biocompatibility of 50LP10 MSP in direct contact with cells, PK-84, HK-2 and PTEC cells (15,000 cells/cm^2) were co-seeded with 5 µm MSP, 30 µm MSP or polydisperse MSP (0.1 mg/600 µL complete medium). Similarly, the three cell types were co-incubated

with Poly Urethane Film made from 2365-55D- pellethane resin (Dow Chemical, Midland, MI, USA) by Medtronic Promeon (Minneapolis, MN, USA) as a control for excellent biocompatibility, or rubber latex (Hilversum Rubber Factory, Hilversum, The Netherlands) as a control for poor biocompatibility (leading to rapid cell death). Both controls were previously used in toxicology studies (De Groot et al., 2001). Cultures were maintained for 72h. Cell morphology was examined microscopically every day. After 72 h, mitochondrial activity and cell proliferation was assessed, as described below.

To test the biocompatibility of possible leachables or early degradation products from the polymer 50LP10 (see above), PK-84, HK-2 and PTEC cells were seeded in 24-well plates at a cell density of 15,000 cells/cm^2. After 24h, medium was replaced with medium containing leachables or degradation products from 50LP10, polyurethane or latex, and cells were cultured for another 48h. Cell morphology was examined every day. After 48h, mitochondrial activity and cell proliferation was assessed, as described below.

Mitochondrial activity assay

Cell viability was determined by assessing mitochondrial activity, using the CellTiter 96® AQueous One Solution Cell Proliferation Assay (MTS assay, Promega Benelux BV, Leiden, The Netherlands), according to manufacturer's instructions. Briefly, cells were washed and MTS solution was added to each well and incubated for 2 h at 37 °C. Absorbance was read at 490 nm using a fluorescence microplate reader (Varioscan, Thermo Fisher Scientific Inc.).

Cell proliferation assay

Cell proliferation was determined by cellular DNA content, using the CyQUANT assay (Invitrogen, Breda, The Netherlands), according to the manufacturer's instructions. Briefly, culture medium (including floating and dead cells) was removed and remaining, viable cells were stored at -80°C. Subsequently, culture plates were thawed at room temperature and lysis buffer, demineralized water and CyQUANT GR dye stock solution were added to each well. Plates were incubated for 5 min. in the dark and fluorescence was measured with a fluorescence microplate reader (Varioscan, Thermo Fisher Scientific Inc.), with filters appropriate for 480 nm excitation and 520 nm emission.

Assessment of bioburden in 50LP10 MSP

Potential bacterial contamination in the MSP preparations was assessed by inoculation of MSP on blood agar plates and incubation at 37°C for 4 days. The presence of bacterial colonies was checked daily. Moreover, 1 mg of MSP was suspended in complete culture medium, without addition of penicillin and streptomycin, and incubated at 37°C, 5% CO_2 for 7 days. Medium was checked daily for bacterial growth. Endotoxin levels were determined using the *limulus* Amebocyte Lysate (LAL) assay performed by Toxikon (Toxikon Europe NV, Leuven, Belgium) and were well under the accepted FDA limits (0.5 EU/mL) for medical devices.

Animals and implantation procedures

F344 (Harlan Laboratories, Inc. Hillcrest, Great Britain) rats weighing 240 ± 50 g were fed laboratory chow and acidified water ad

libitum, and were housed according to institutional rules in groups of three till five, with 12:12 hours dark light cycles. The Animal Ethical Committee of the University of Groningen approved the experimental protocol. All operations were performed under general isoflurane/O_2 inhalation anesthesia.

MSP were resuspended in an aqueous reconstitution medium containing 0.4 w/v% CMC at a ratio of 20 mg MSP/150 µl CMC and injected subcutaneously on the back of rats (n=3/group/time point) using a 20G needle for the monodisperse MSP and an 18G needle for the polydisperse MSP (Terumo Europe N.V. Leuven, Belgium). MSP implants and surrounding tissue were explanted after 7, 14 and 28 days.

For subcapsular implantations, an abdominal incision was made and two subcapsular pockets were generated on the left kidney, in which either, 30µm mMSP, or polydisperse MSP were injected (5 mg MSP/pocket n=5/group/time point). Kidneys were flushed with saline and all implants were fixed in Zink fixative (0.1 M Tris-buffer, 3.2 mM calcium acetate, 23 mMZink acetate, 37 mM zinc chloride, pH 6.5–7.0; Merck) overnight, prior to paraffin embedding. Implants were cut into 4.0 µm-thick sections.

(Immuno)histochemistry

General histologic assessment of the FBR towards 50LP10 MSP was based on toluidine blue staining (FlukaChemie, Buchs, Switzerland), according to a standard staining protocol. Tissue sections were mounted in permount (Fisher Scientific International) and inspected microscopically.

Macrophages were identified by immunohistochemical detection of ED-1. Briefly, sections were deparaffinized and antigen retrieval was

performed overnight in a 0.1 M Tris-HCl buffer at 80°C. Sections were incubated in mouse-anti-rat ED-1 monoclonal antibody for 1 h (10 μg/mL; MCA341R, AbDSerotec, Dusseldorf, Germany) and, subsequently, in horseradish peroxidase-conjugated rabbit-anti-mouse polyclonal antibody for 30 min (13 μg/mL; DAKO, Glosstrup, Denmark). Enzyme activity was developed using 3-amino-9-ethylcarbazole (AEC; Sigma-Aldrich, Zwijndrecht, The Netherlands) as a substrate. Washing and blocking of aspecific binding sites and endogenous peroxidase was performed according to standard procedures. Sections were mounted in Kaisersglycerine.

Myofibroblasts and blood vessels were detected by immunohistochemical staining for alpha smooth muscle actin (αSMA). Briefly, slides were deparaffinized and antigens were retrieved overnight in a 0.1 M Tris-HCl buffer at 80°C. Tissue sections were incubated in mouse αSMA monoclonal antibody (Clone 1A4; 0.44 μg/mL; DAKO) for 1 h. Subsequently, tissue sections were washed and endogenous peroxidase was blocked with a 0.1% H_2O_2/PBS solution for 10 min. Finally, sections were incubated in horseradish-conjugated rabbit-anti-mouse polyclonal antibody (13 μg/mL; DAKO) for 30 min., rinsed in PBS, incubated with AEC and finally mounted in Kaisersglycerine.

Connective tissue was visualized by Masson trichrome staining. Briefly, sections were deparaffinized and fixed in bouin fixative for 4 min at 51°C. Slides were stained with Weighert's iron hematoxyline for 10min., rinsed with 37°C tap water (10 min) and stained with Biebrich scarlet-acid fuchsin solution (15 min). Sections were differentiated in phosphomolybdic-phosphotungstic acid solution (15 min), washed, and stained with aniline

blue solution (10 min). Finally, sections were differentiated in 1% acetic acid solution (10 sec), washed, dehydrated quickly by dipping in alcohol followed by xylene, and mounted in permount (Thermo Fisher Scientific Inc. Breda, The Netherlands). Sections were washed in demi-water between incubation steps, unless otherwise indicated. To confirm ECM deposition, with a focus on collagens, we performed a Picrosirius Red staining. Briefly, sections were deparaffinised, rehydrated and stained with picro-sirius red solution for 1 h. After washing twice with acidified water (0.5% v/v acetic acid glacial in demi water), sections were dehydrated quickly (see above) and mounted in permount.

Quantifications

Stainings were evaluated using a Leica DM 2000 microscope. For morphometric quantifications, five representative photomicrographs within implants were taken per tissue section, using a Multispectral Imaging Camera (PerkinElmer, Groningen, The Netherlands). Photomicrographs were analyzed using Nuance 3.0 software (Perkin Elmer), which allows exquisite detection of specific signal (stained area) without interference of background noise. Stained areas were quantified for each specific staining and expressed as average surface area in square micrometer per high power field (HPF). Cellularity was quantified by digital counting of nuclei in photomicrographs of toluidine-blue stained sections. MSP diameters were determined by measuring 50 MSP per implant using an Olympus BX50 camera (Olympus, Tokyo, Japan) with Cell^B software (Olympus Soft Imaging Solution GmbH, Münster, Germany).

Statistics

Statistical differences between groups were determined using a two-way ANOVA, followed by Bonferroni post hoc analysis, using GraphPad Prism version 5 (GraphPad Software, La Jolla, USA). P values < 0.05 were considered to be statistically significant. Data are shown as mean ± standard error of the mean (SEM).

Results

In vitro biocompatibility of 50LP10 MSP

Cytotoxicity studies were performed on 3 cell types; PK-84, a fibroblast cell line and HK-2 and PTEC cells, as organotypic cell types which are both present in the kidney. All cytotoxicity studies were compared to negative control poly-urethane (PU), which did not affect any of the parameters, and positive control latex, which resulted in cell death in all cell types studied. Cells were exposed both to direct contact with the materials and to extracted leachables. Since these results were very similar, we report here only the data from direct contact.

Based on their morphology PK-84, HK-2 and PTEC cells were not influenced by direct contact to, or leachables from, 50LP10 MSP of any size (Fig 1 B-C; G-H; L-M & data not shown respectively). Negative control poly-urethane (PU) did not influence the cell morphology in either the direct contact or the exposure to leachables (Fig 1 D, I, N & data not shown). Exposure to positive control latex in direct contact or as leachables however resulted in a disrupted monolayer in HK-2 and PTEC cells and a strongly altered cell morphology in PK-84 cells (Fig 1 E, J, O

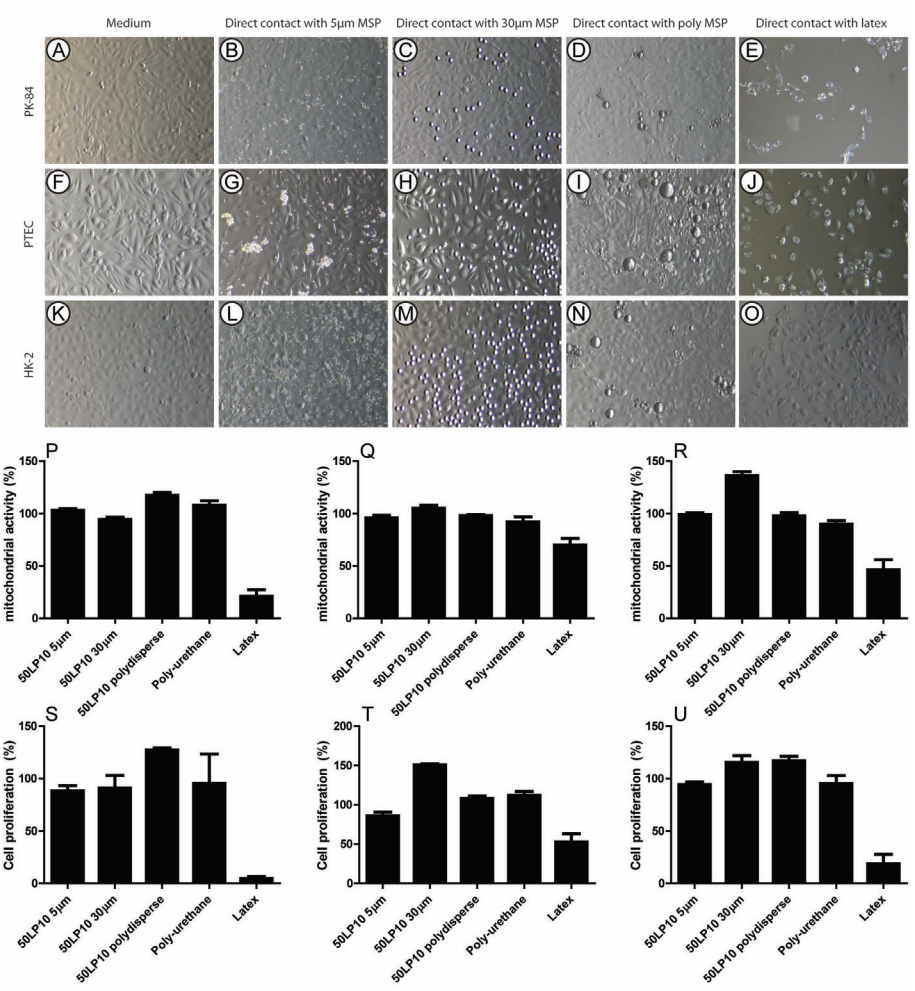

Figure 1. *In vitro* biocompatibility of 50LP10 MSP. PK-84, PTEC and HK-2 cells were cultured for 72 h in medium (A, F, K) in direct contact with 5 µm PLGA MSP (B, G, L), 30 µm PLGA MSP (C, H, M), polydisperse PLGA MSP (D, I,N), polyurethane (not shown), or in latex (E,J,O). Mitochondrial activity was measured using the CellTiter 96 Aqeous one Solution Assay (P, Q, R) and cell proliferation was determined using the CyQuant cell proliferation assay (S, T, U). Bars represent mean values and SEM.

& data not shown). Exposure to rubber latex in direct contact or exposure to leachables also clearly resulted in cell death in all cell types.

Since mitochondrial activity might be altered in absence of any morphological changes we assessed mitochondrial activity in each of the cell types. Cell culture in direct contact with 50LP10 MSP of any size did not have a negative effect upon the metabolic activity of any of the cell types. Direct contact with negative control PU, as expected, also did not negatively influence the mitochondrial activity. However, direct contact with positive control rubber latex resulted in a significant decrease in mitochondrial activity in all three cell types (Figure 1 P, Q, R). Similar results were obtained after exposing these three cell types to leachables of 50LP10 MSP (data not shown).

Since exposure of cells to 50LP10 MSP might negatively affect cell proliferation or induce increased cell death we measured DNA content. Here, we obtained similar results as those observed in the mitochondrial activity study. Direct contact of these three cell types with 50LP10 MSP of any size did not negatively influence cell proliferation. Direct contact between negative control PU and any of the cell types also did not influence the cell proliferation, but upon direct contact with positive control, rubber latex, the cell proliferation was significantly decreased (figure 1 S, T, U). Similar results were obtained after exposure of the three cell types to leachables of 50LP10 MSP and the controls (data not shown).

Cellular infiltration

Cellular infiltration, in particular of macrophages, is a major factor in the FBR. To obtain a first impression of the effect of MSP size on the FBR,

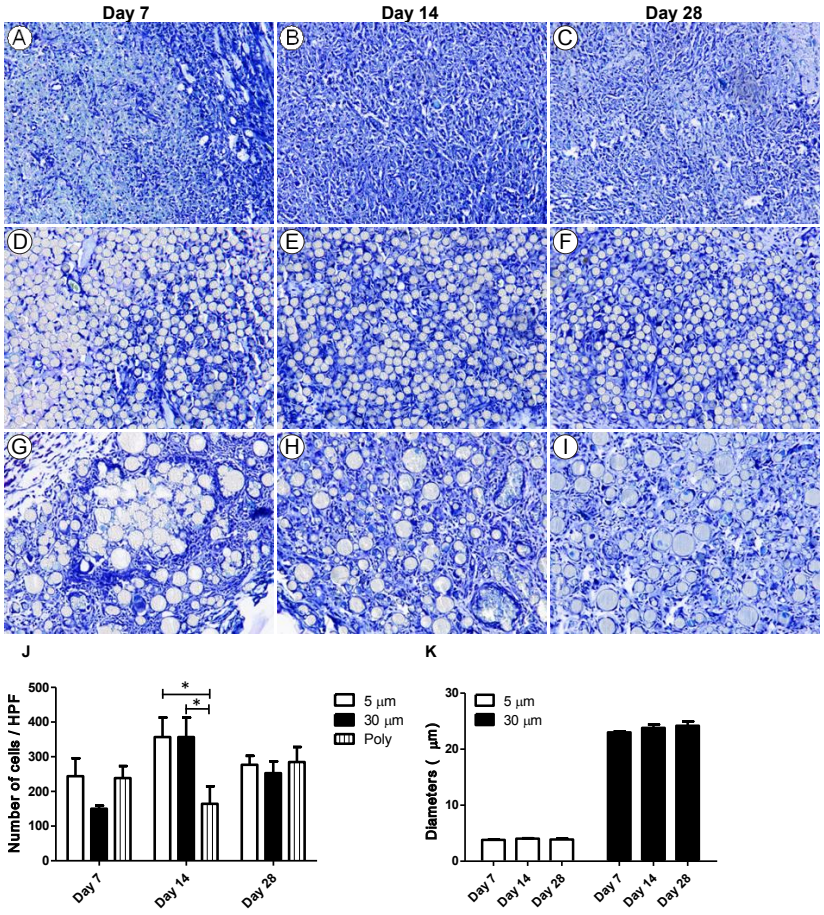

Figure 2. Cellular influx and MSP degradation. PLGA MSP with a diameter of 5 µm (A-C), 30 µm (D-F) and polydisperse MSP (G-I) were injected subcutaneously and explanted at day 7, 14 or 28. Cell influx was determined by morphometry (K) and average sphere diameter was calculated for each time point (K). Scale bars represent 100µm. Bars represent mean values and SEM. * P<0.05. HPF: high power field.

we investigated the effect of MSP size on cellular infiltration. Infiltrating cells were present at all time points (figure 2A-I) and there were no striking differences in amount of cellular infiltration at all time points between MSP sizes. The only exception was day 14, where cellular infiltration between polydisperse MSP was significantly lower than between 5 and 30μm MSP (figure 2K). However, this difference disappeared on day 28 when cellular infiltration between the different MSP groups was comparable. We did not observe any lymphocytes or polymorphonuclear cells, based on nuclear morphology, suggesting that the vast majority of inflammatory infiltrating cells consisted of macrophages.

Microsphere characteristics

After subcutaneous injection of the MSP in rats, we first confirmed the monodispersity of the mMSP groups. *In vivo* the mMSP were smaller than expected: 30 μm mMSP were on average 23.4 μm and 5 μm mMSP were 3.9 μm. Although the size was lower than expected the mMSP maintained the same size *in vivo* during the entire study with very low standard deviations (figure 2J).

Macrophage infiltration

To confirm this morphological finding we performed an ED-1 staining, which identifies macrophages (figure 3 A-I). Interestingly, small 5 μm mMSP implants contained more ED-1 positive macrophages at all time points compared to 30 μm and polydispersemMSP implants. Furthermore, the macrophage response in time towards the three MSP groups was different as well. Macrophage infiltration reached its maximum

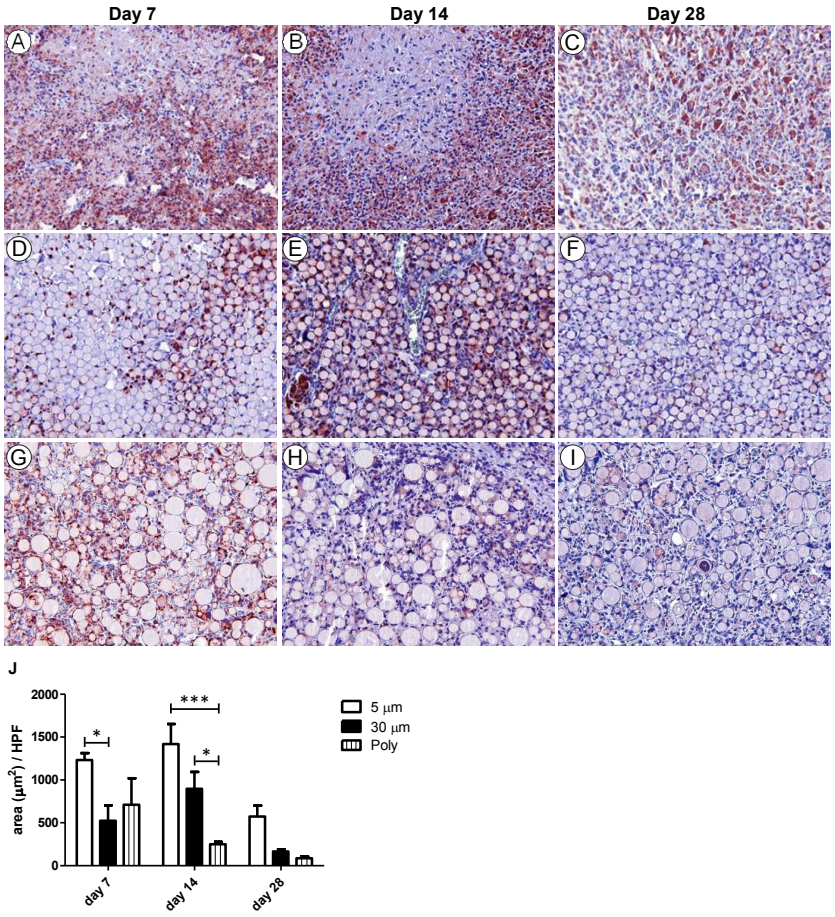

Figure 3. Macrophage infiltration. 50LP10 MSP with a diameter of 5 µm (A-C), 30 µm (D-F) and polydisperse MSP (G-I) were injected subcutaneously and explanted at day 7, 14 or 28. Average ED-1-stained area is shown in J. Data represents mean values and SEM. HPF: high power field. * P<0.05, ***P<0.001

on day 7 in the polydisperse group, but only peaked at day 14 in the monodisperse groups. At day 28 macrophage infiltration was diminished in all groups, suggesting a decreasing inflammatory response against the MSP, this decreased inflammatory response at day 28 was more pronounced in the polydisperse and 30 µm groups.

Macrophage behavior

To optimally predict the usefulness of these mMSP as a drug delivery device it is important to know how cells, and specifically macrophages, will respond towards these mMSP. Therefore we took a closer look at where the macrophages were located and how they interacted with the foreign body material. As noted above, all implants contained macrophages, irrespective of mMSP size. However, we found that 5 μm mMSP were phagocytosed, whereas 30 μm mMSP were not (figure 4A-B). In figure 4A we clearly show white spheres (5 μm mMSP) located in red stained cells (ED-1 staining), indicating that these mMSP were phagocytosed. On the other hand, in figure 4B we show that macrophages infiltrating the 30 μm mMSP implants are all located solely between the mMSP. We did not observe any phagocytosed 30 μm mMSP. Within the polydisperse MSP group we observed that small MSP (<10 μm) were phagocytosed where the larger MSP(>20 μm) were not.

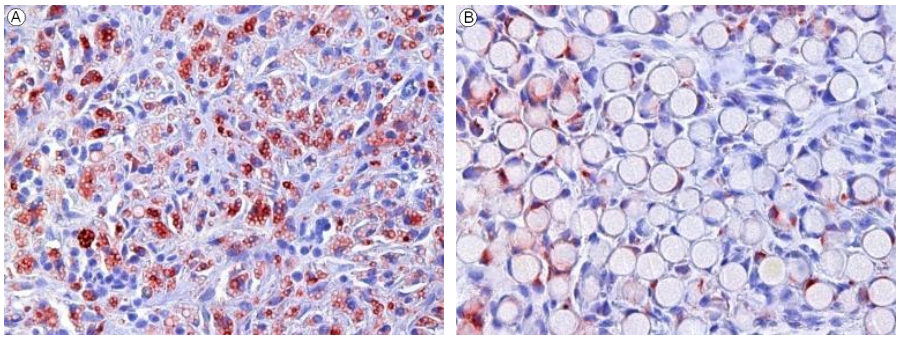

Figure 4. Macrophage behaviour in relation to MSP size. 50LP10 MSP with a diameter of 5 μm (A) and 30 μm (B) were injected subcutaneously and explanted at day 7. Macrophages phagocytize small (5 μm) MSP, as shown by MSP location inside ED-1-stained area, while they attached to large (30 μm) MSP.

Myofibroblast infiltration/encapsulation

Myofibroblasts, a well-known hallmark of the foreign body response (FBR), may form a fibrous capsule around the implant, influencing its function. Myofibroblasts are characterized by the expression of α-SMA. Upon staining for this protein, we found that the explants containing small 5 μm mMSP were partially encapsulated by myofibroblasts, which can negatively influence drug release. Large 30 μm mMSP and polydisperse MSP were not encapsulated at all (figure 5).

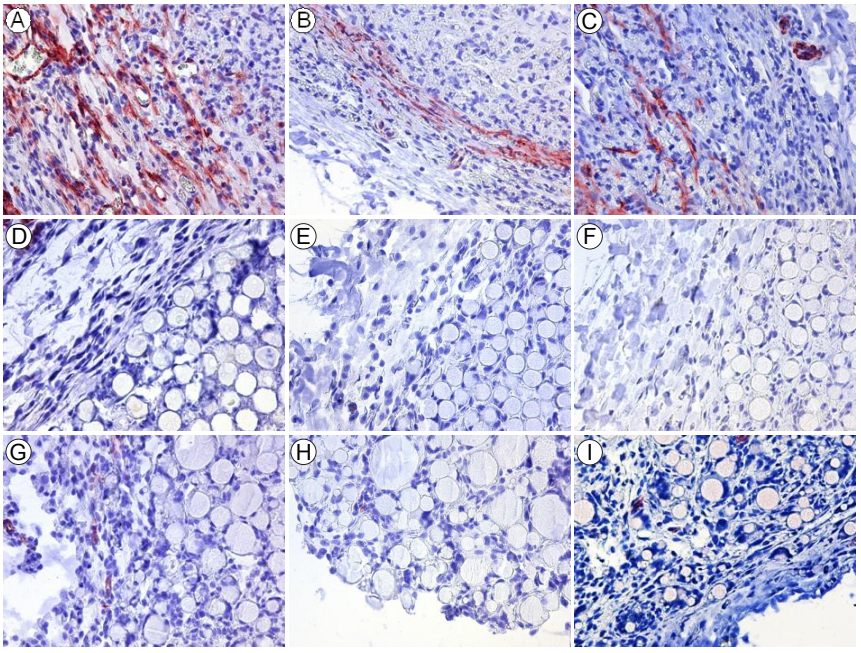

Figure 5. Assessment of implant encapsulation by myofibroblasts. 50LP10 MSP with a diameter of 5 μm (A-C), 30 μm (D-F) and polydisperse MSP (G-I) were injected subcutaneously and explanted at day 7, 14 or 28. Myofibroblasts were detected by smooth muscle actin staining.

Implant vascularization

Vascularization of implants can also influence the FBR, and can be quantified by staining for α-smooth muscle actin (α-SMA), which also stains smooth muscle cells present in vessel walls. Based on this staining, on day 7 and 14 we observed that small mMSP increase vascularization but this effect is diminished on day 28. There was no difference in vascularization between 30 µm mMSP and polydisperse MSP implants at any time point (figure 6 A-D).

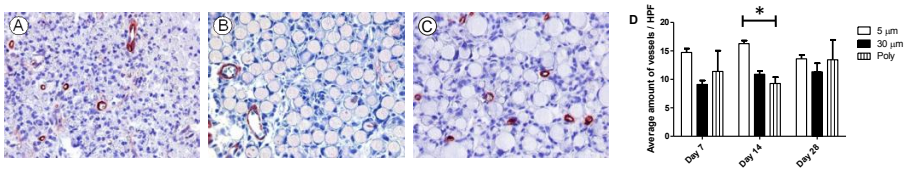

Figure 6. Vascularization in 50LP10 MSP implants. 50LP10 MSP with a diameter of 5 µm (A), 30 µm (B) and polydisperse MSP (C) were injected subcutaneously and explanted at day 7. Blood vessels were detected by smooth muscle actin staining of vascular smooth muscle cells. Blood vessels were counted manually (D). Bars represents mean values and SEM. HPF: high power field.

ECM/collagen deposition

Increased ECM deposition is not only a hallmark of the FBR but also negatively influences the function of a drug delivery device and it is therefore important to induce this increase to a minimum amount. MSP size influenced the amount of collagens deposited during the FBR, as can be seen in the Masson Trichrome staining (figure 7 A-I). Small mMSP clearly caused enhanced connective tissue deposition (indicated in blue), compared to the amount of connective tissue that was deposited between large and polydisperse MSP. The Masson Trichrome staining was difficult to quantify. Therefore we performed a picrosirius staining in

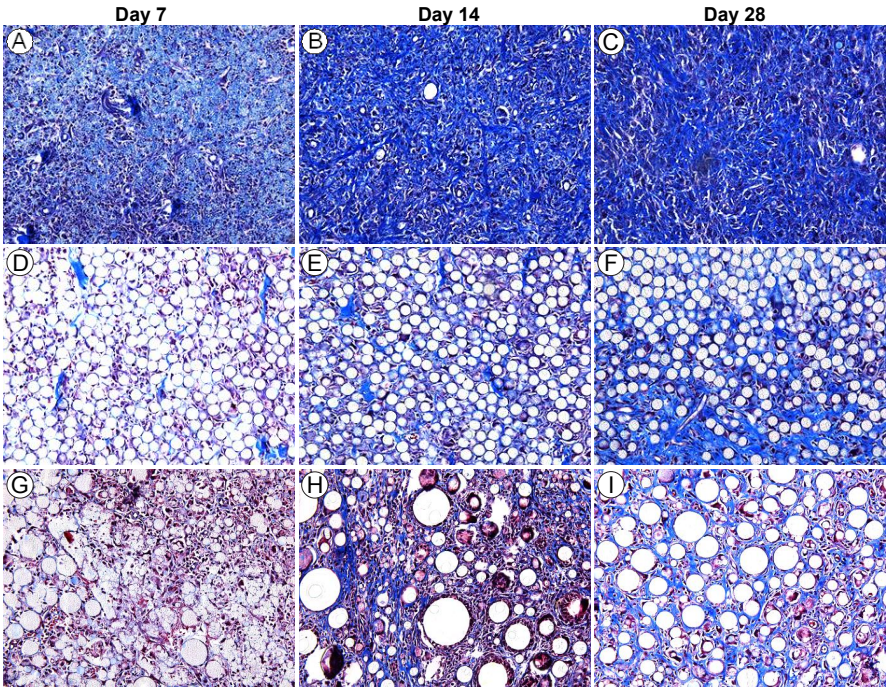

Figure 7. Extracellular matrix deposition in PLGA MSP implants. PLGA MSP with a diameter of 5 µm (A-C), 30 µm (D-F) and polydisperse MSP (G-I) were injected subcutaneously and explanted at day 7, 14 or Masson trichrome staining was used to visualize extracellular matrix (ECM) deposition (blue dye).

which the deposited collagen is shown in red (figure 8). There was an increased deposition of collagens between 5 µm mMSP at all three time points compared to 30 µm mMSP. We found no differences in collagen deposition between 30 µm mMSP and polydisperse MSP, except for day 7, where collagen deposition was significantly lower in the 30 µm explants.

Mild FBR against subcapsular implanted MSP

Based on their good biocompatibility in the subcutaneous FBR model, we chose 30 µm and polydisperse MSP for injection underneath the kidney capsule. This is an attractive site for local drug delivery in

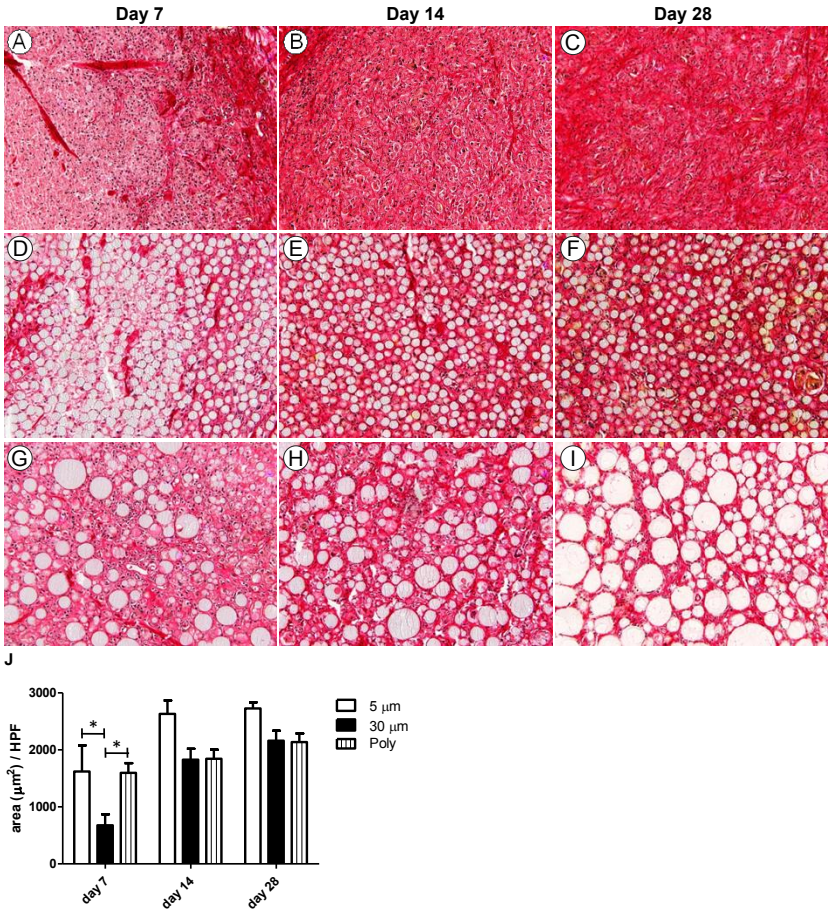

Figure 8. Detection and quantification of total collagen deposition by Picro Sirius Red staining. 50LP10 MSP with a diameter of 5 µm (A-C), 30 µm (D-F) and polydisperse MSP (G-I) were injected subcutaneously and explanted at day 7, 14 or 28. Total collagen deposition in implants was determined by Picrosirius Red staining and quantified by morphometry of stained area (J). Bars represents mean values and SEM. HPF: high power field.

kidney disease, because it consists of an area between the kidney cortex and the kidney capsule where a drug delivery device can be injected without harming kidney cells. We show in figure 9A that 30 µm mMSP were distributed more evenly under the kidney capsule, thereby increasing the therapeutic range compared to polydisperse MSP. This is evidenced

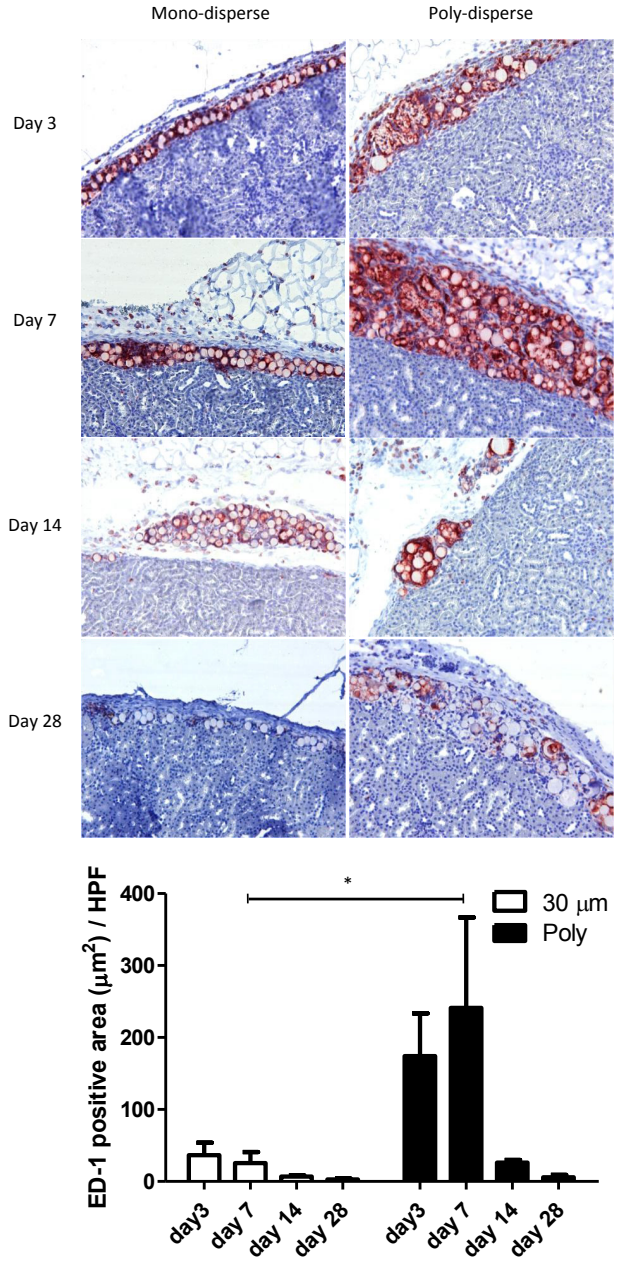

Figure 9. Macrophage infiltration. 50LP10 MSP with a diameter of 30 μm and polydisperse MSP were injected underneath the kidney capsule and explanted at day 3, 7, 14 and 28. Average ED-1-stained area is shown in the graph. Data represents mean values and SEM. HPF: high power field. * $P<0.05$.

by there being at most one or two layers of microspheres between the kidney cortex and the kidney capsule in the 30 μm mMSP group, where polydisperse MSP stick to one another to such an extent that a layer of 10 MSP thick may be formed.

Macrophages play an important role in kidney disease and therefore we started by examining ED-1 positivity in the kidney cortex. MSP injected underneath the kidney capsule did not trigger or attract macrophages in the kidney cortex, irrespective of their size. Furthermore, 30 μm mMSP evoked a milder inflammatory response in the subcapsular space, since the amount of the ED-1 staining between the MSP was decreased compared to polydisperse MSP, especially on day 3 and 7 (figure 9B).

Myofibroblast formation in the kidney capsule

No α-SMA positive cells were observed in the kidney cortex in any time point (figure 10A). The kidney capsule however was positive for α-SMA, suggesting the presence of myofibroblasts there. Although not significantly, the number of myofibroblasts in the capsule decreased faster in 30 μm mMSP than in polydisperse MSP (figure 10B).

Discussion

The goal of this work was to produce a well-characterized, biocompatible microsphere formulation, of three distinct different sizes, and investigate whether the size of the 50LP10 microspheres influences the FBR. As an advantage over conventional PLGA this polymer is suitable for releasing proteins. Secondly, we wanted to investigate whether local drug delivery in the kidney with microspheres is possible without harming

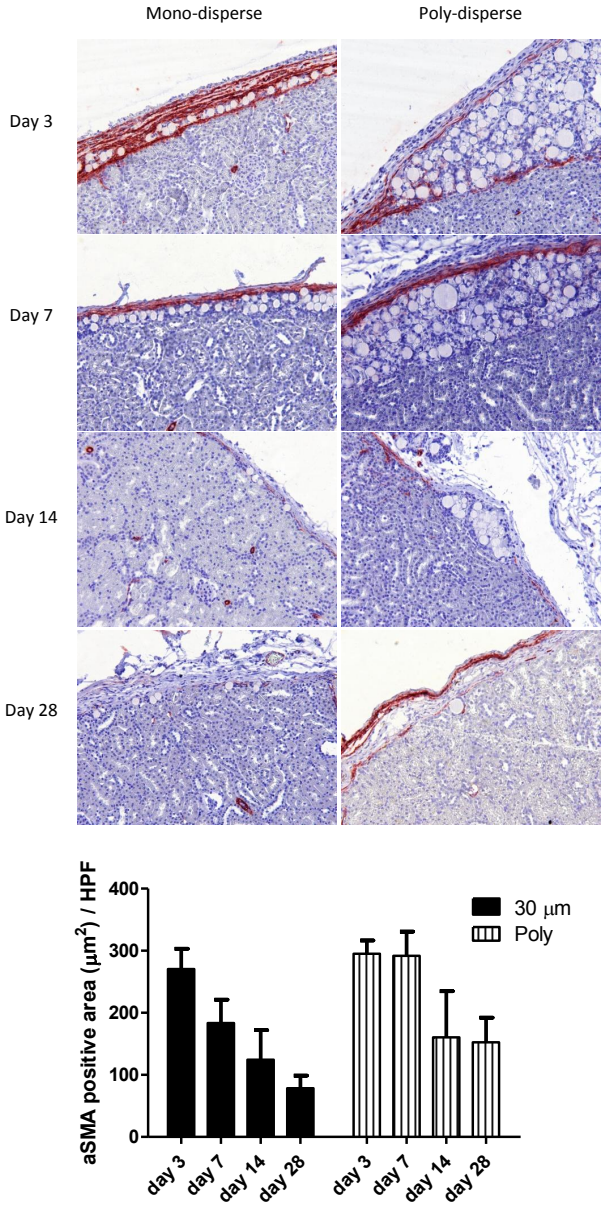

Figure 10. Assessment of implant encapsulation by myofibroblasts. Monodisperse 50LP10 MSP with a diameter of 30 µm and polydisperse MSP were injected subcutaneously and explanted at day 3, 7, 14 and 28. Average aSMA stained area is shown in the graph. Data represents mean values and SEM. HPF: high power field.

kidney cells. First of all we confirmed *in vitro* biocompatibility, in three different cell types, based on morphology, mitochondrial activity and DNA content. We used this method previously [16] and it seems to be a promising tool in selecting biomaterials for *in vivo* use.

Based on our previous findings we expected that monodisperse 30µm mMSP would be superior compared to 5µm mMSP and polydisperse MSP based on biocompatibility and capacity to release a drug to a local environment without being phagocytosed by macrophages. In this study we confirmed this expectation, suggesting that our previous conclusion that MSP size influences the FBR [16] is solid, and not dependent on the chemistry or material of the MSP. The findings between both studies are comparable, although the overall FBR towards 50LP10 was slightly stronger compared to PLGA. This was mainly seen by an increased macrophage infiltration and myofibroblast accumulation. The small 5µm mMSP in particular were partly encapsulated by myofibroblasts, indicating that this size of mMSP is less well tolerated by the body in general. This increased FBR against smaller particles has also been proposed by Zardeneta *et al.* who suggest that the biological response is strongly related to the particle size of polytetrafluoroethylene [17]. The differences in FBR against 50LP10 and PLGA however might be explained by various factors, such as the difference in chemistry, the degradation process of the polymer or a difference in batches of carrier CMC used in these studies.

Apart from the comparable FBR between PLGA and 50LP10 MSP, we also saw the same macrophage behavior against the two types of MSP. In both cases small 5µm mMSP were phagocytosed whereas large 30µm

mMSP were not, which confirms the study of Champignon *et al.* [18], who found that 2-3 μm MSP were easily phagocytosed and larger MSP were increasingly difficult to phagocytose.

We hypothesize that the process of phagocytosis might be responsible for the differences seen in the extent of the FBR against the different sizes of MSP. It is known that phagocytic stimuli increase ED-1 positivity in macrophages [19]. This increase in ED-1 positivity can lead to increased cytokine expression, which in turn activates fibroblasts to become myofibroblasts, which are well known for their capacity to deposit collagens [20]. This process might be the reason for the observed increase in deposition of extracellular matrix in implants of 5 μm mMSP.

Surprisingly, we did not observe many differences between polydisperse MSP and 30μm mMSP subcutaneously. We expect that the size distribution of the polydisperse MSP might be responsible for this, since the overall size of the polydisperse MSP was more close to 30 μm mMSP than 30 μm mMSP. When we continued our experiments with these two best MSP formulations and injected these underneath the kidney capsule, the 30μm mMSP appeared to perform better compared to polydisperse MSP. First of all the mMSP distributed more evenly underneath the kidney capsule, which increased the therapeutic range of the drug delivery vehicle. Secondly, less macrophage infiltration was observed between the 30μm mMSP compared to the polydisperse MSP. More experiments need to be performed to investigate why the FBR against polydisperse MSP is stronger in a subcapsular FBR model compared to a subcutaneous model. A possible explanation for the differences observed subcapsularly is that

monodisperse 30µm mMSP were easily injected underneath the kidney capsule whereas polydisperse MSP required a larger needle size. This may have resulted in increased damage to the kidney capsule as indicated by the continued presence of myofibroblasts and prolonged time to recovery.

Most importantly, for a successful local drug delivery device used in the kidney, the device itself should not damage or harm the kidney in any way. It is important to note that subcapsular MSP injections did not harm the kidney cortex in any way, based on the absence of macrophages and myofibroblasts. Therefore, local drug delivery by 50LP10 mMSP seems promising. Due to its more favorable chemistry it should be an alternative for PLGA which can be used for delivery of proteins and other compounds which cannot be incorporated in PLGA microspheres as previously mentioned. In contrast to conventional systemic drug delivery, local drug delivery to the kidneys can reduce side effects by reducing systemic and/or non-renal exposure to the drugs. Furthermore, compared to systemically delivered drugs, locally delivered drugs can have the same or greater therapeutic effect in lower quantities and/or concentrations [21,22].

In summary, we conclude that both mMSP and polydisperse MSP were well tolerated by the kidney. However, the mMSP were more evenly distributed underneath the kidney capsule, evoked a milder macrophage response, and the kidney capsule recovered faster from the operating procedure. Although PLGA is a well-known biocompatible drug releasing platform, the degradation of this polymer (into lactic and glycolic acid) hampers its possibilities for releasing proteinaceous drugs, since many proteins lose their activity in an acidic environment. Therefore we

developed a new polymer which evokes a comparable FBR compared to PLGA and is a better candidate for local protein drug delivery.

Acknowledgments

This research forms part of the Project P3.02 DESIRE of the research program of the BioMedical Materials institute, co-funded by the Dutch Ministry of Economic Affairs.

References list

1. Kim SJ, Park JG, Kim JH, Heo JS, Choi JW, Jang YS, et al. Development of a biodegradable sirolimus-eluting stent coated by ultrasonic atomizing spray. J Nanosci Nanotechnol 2011 Jul;11(7):5689-5697.
2. Shmueli RB, Ohnaka M, Miki A, Pandey NB, Lima e Silva R, Koskimaki JE, et al. Long-term suppression of ocular neovascularization by intraocular injection of biodegradable polymeric particles containing a serpin-derived peptide. Biomaterials 2013 Oct;34(30):7544-7551.
3. Xuan J, Lin Y, Huang J, Yuan F, Li X, Lu Y, et al. Exenatide-loaded PLGA microspheres with improved glycemic control: in vitro bioactivity and in vivo pharmacokinetic profiles after subcutaneous administration to SD rats. Peptides 2013 Aug;46:172-179.
4. Menon JU, Ravikumar P, Pise A, Gyawali D, Hsia CC, Nguyen KT. Polymeric nanoparticles for pulmonary protein and DNA delivery. Acta Biomater 2014 Jun;10(6):2643-2652.
5. Reguera-Nunez E, Roca C, Hardy E, de la Fuente M, Csaba N, Garcia-Fuentes M. Implantable controlled release devices for BMP-7 delivery and suppression of glioblastoma initiating cells. Biomaterials 2014 Mar;35(9):2859-2867.
6. Wink JD, Gerety PA, Sherif RD, Lim Y, Clarke NA, Rajapakse CS, et al. Sustained delivery of rhBMP-2 by means of poly(lactic-co-glycolic acid) microspheres: cranial bone regeneration without heterotopic ossification or craniosynostosis. Plast Reconstr Surg 2014 Jul;134(1):51-59.
7. Huang SS, Li IH, Hong PD, Yeh MK. Development of Yersinia pestis F1 antigen-loaded microspheres vaccine against plague. Int J Nanomedicine 2014 Feb 7;9:813-822.
8. Joshi VB, Geary SM, Salem AK. Biodegradable particles as vaccine antigen delivery systems for stimulating cellular immune responses. Hum Vaccin Immunother 2013 Dec;9(12):2584-2590.
9. Spenlehauer G, Vert M, Benoit JP, Boddaert A. In vitro and in vivo degradation of poly(D,L lactide/glycolide) type microspheres made by solvent evaporation method. Biomaterials 1989 Oct;10(8):557-563.
10. Vert M, Mauduit J, Li S. Biodegradation of PLA/GA polymers: increasing complexity. Biomaterials 1994 Dec;15(15):1209-1213.
11. Estey T, Kang J, Schwendeman SP, Carpenter JF. BSA degradation under acidic conditions: a model for protein instability during release from PLGA delivery systems. J Pharm Sci 2006 Jul;95(7):1626-1639.

12. Crotts G, Park TG. Protein delivery from poly(lactic-co-glycolic acid) biodegradable microspheres: release kinetics and stability issues. J Microencapsul 1998 Nov-Dec;15(6):699-713.
13. Hermeling S, Crommelin DJ, Schellekens H, Jiskoot W. Structure-immunogenicity relationships of therapeutic proteins. Pharm Res 2004 Jun;21(6):897-903.
14. Patten PA, Schellekens H. The immunogenicity of biopharmaceuticals. Lessons learned and consequences for protein drug development. Dev Biol (Basel) 2003;112:81-97.
15. Wolinsky JB, Colson YL, Grinstaff MW. Local drug delivery strategies for cancer treatment: gels, nanoparticles, polymeric films, rods, and wafers. J Control Release 2012 Apr 10;159(1):14-26.
16. Zandstra J J. Microsphere size influences the foreign body reaction. European Cells and Materials 2014;28:335-47.
17. Zardeneta G, Mukai H, Marker V, Milam SB. Protein interactions with particulate Teflon: implications for the foreign body response. J Oral Maxillofac Surg 1996 Jul;54(7):873-878.
18. Champion JA, Walker A, Mitragotri S. Role of particle size in phagocytosis of polymeric microspheres. Pharm Res 2008 08;25(0724-8741; 0724-8741; 8):1815-1821.
19. Damoiseaux JG, Dopp EA, Calame W, Chao D, MacPherson GG, Dijkstra CD. Rat macrophage lysosomal membrane antigen recognized by monoclonal antibody ED1. Immunology 1994 Sep;83(1):140-147.
20. Clark RA. Regulation of fibroplasia in cutaneous wound repair. Am J Med Sci 1993 Jul;306(1):42-48.
21. Arruebo M, Vilaboa N, Santamaria J. Drug delivery from internally implanted biomedical devices used in traumatology and in orthopedic surgery. Expert Opin Drug Deliv 2010 May;7(5):589-603.
22. Windecker S, Roffi M, Meier B. Sirolimus eluting stent: a new era in interventional cardiology? Curr Pharm Des 2003;9(13):1077-1094.